Artvin Çoruh Üniversitesi
Doğal Afetler Uygulama ve Araştırma Merkezi
Doğal Afetler ve Çevre Dergisi

Artvin Çoruh University
Natural Hazards Application and Research Center
Journal of Natural Hazards and Environment

Araştırma Makalesi / Research Article, Doğ Afet Çev Derg, 2025; 11(1): 157–169, DOI: 10.21324/dacd.1495772

The Impact of River Mouth Sediment Deposition on Flood Risk: The Case Study of The Sakarya River

Osman Sönmez[1,*], Temel Temiz[2], Beytullah Demirci[3]

[1]*Department of Civil Engineering, Sakarya University, Esentepe Campus, 54050, Sakarya.*
[2]*Department of Civil Engineering, Yalova Üniversitesi, Central Campus, 77200, Yalova.*
[3]*Floodis Engineering, Project Desing and Consultancty Ltd., Ankara.*

Abstract

Flooding is a natural disaster that causes loss of life and property worldwide. Floods can be predicted and their damages can be reduced. Various natural and man-made factors can cause floods. Sediment movement can be counted as one of the causes of floods, albeit rarely. The Sakarya River bed and river mouth is one of the risky areas for flooding due to sediment deposition. Due to the activities of quarries on the Sakarya River, the amount of sediment carried by the river increases, and the damage to the river bed morphology. In rare cases, the mouth of the river is completely closed due to sedimentation, which has caused many disasters such as coastal flooding and capsizing of marine vessels, leading to loss of life and property. Therefore, the occurrence of floods due to sediment deposition at the mouth of Sakarya River was investigated. The 5, 10, 25, 50, 100, and 500-year return period flows in the downstream part of the Sakarya River and Karasu district were analyzed with the 2D flood model in case of insufficient discharge from the river mouth. Water depth, velocity, and flood hazard maps for these return periods were prepared. The impact of flooding on Karasu district was analyzed in terms of affected buildings and affected area (ha). Thus, the effects of the floods occurring in the downstream region as a result of the interventions to the river bed in the upstream region were analyzed.

Keywords

Sakarya River, Sediment, Flood, Depth, Hazard

Nehir Ağzı Sediment Birikiminin Taşkın Riskine Etkisi: Sakarya Nehri Örneği

Özet

Taşkın, dünya çapında can ve mal kaybına neden olan doğal bir afettir. Taşkınlar tahmin edilebilir ve zararları azaltılabilir. Çeşitli doğal ve insan kaynaklı faktörler taşkınlara neden olabilir. Sediment hareketi nadiren de olsa taşkınların nedenlerinden biri olarak sayılabilir. Sakarya Nehri yatağı ve nehir ağzı, sediment birikimi nedeniyle taşkınlar için riskli alanlardan biridir. Sakarya Nehri üzerindeki taş ocaklarının faaliyetleri nedeniyle nehrin taşıdığı sediment miktarı artmakta ve nehir yatağı morfolojisi zarar görmektedir. Nadiren de olsa sedimantasyon nedeniyle nehir ağzı tamamen kapanmakta, bu durum kıyı taşkınları ve deniz araçlarının alabora olması gibi can ve mal kaybına yol açan birçok felakete neden olmaktadır. Bu nedenle, Sakarya Nehri ağzında sediment birikimine bağlı taşkınların oluşumu araştırılmıştır. Sakarya Nehri'nin mansap kısmında ve Karasu ilçesinde 5, 10, 25, 50, 100 ve 500 yıllık dönüş periyodu akışları, nehir ağzının sediment birikimi sebebiyle yetersiz deşarj olması durumunda 2D taşkın modeli ile analiz edilmiştir. Bu dönüş periyotları için su derinliği, hız ve taşkın tehlike haritaları hazırlanmıştır. Taşkının Karasu ilçesi üzerindeki etkisi, etkilenen binalar ve etkilenen alan (ha) açısından analiz edilmiştir. Böylece memba bölgesinde nehir yatağına yapılan müdahaleler sonucunda mansap bölgesinde meydana gelen taşkınların etkileri analiz edilmiştir.

Anahtar Kelimeler

Sakarya Nehri, Sediment, Taşkın, Derinlik, Tehlike

1. Introduction

Around 1 million people worldwide live in floodplains (Alfieri et al., 2017). This makes the flood a natural phenomenon that many societies should consider. In addition, floods are becoming a more frequent and more widespread problem with climate change. Between 1900 and 2006, floods are approximately one-third of all-natural disasters. The number of people affected by these disasters equals almost half that of those affected by all-natural disasters (Birkholz et al., 2014).

More than half of the world's population lives in cities with rivers and coastlines. The total urban area exposed to flooding in Europe has increased by 1000% over the last 150 years (Jongman, 2018). From the 1950s to the 1990s, the number of floods in European basins increased from 11 to 64 percent, while between 2000 and 2005 there were 104 flood disasters. Flood disaster affects the socioeconomic life of countries and their economic development (Rupal & Agnihotri, 2019).

* Corresponding Author: Tel: +90 (264) 2955713 Faks: +90 (264) 2955601
E-mail: osonmez@sakarya.edu.tr (Sönmez O.), temel.temiz@yalova.edu.tr (Temiz T.) bdemirci@floodis.com (Demirci B.)

Gönderim Tarihi / Received : 04/06/2024
Kabul Tarihi / Accepted : 20/10/2024

The estimated damage caused by flood disasters in Central Europe in 1 year is 16.5 billion dollars (Alphen et al., 2009). In addition to the economic damage and loss of life caused by the flood, there are also effects on the long-term health of the victims (Bubeck et al., 2017).

As in the rest of the world, Turkey has been one of the countries most affected by global climate change. Since it is located on a front where air currents of different pressures and temperatures from Siberia in the north, Africa, and the Arabian Peninsula in the south meet, it is heavily affected by heavy rainfall and the floods that cause it.

In Turkey, flooding is accepted as the riskiest natural disaster due to irregular flow regimes of rivers, geographical location, and geological reasons (Sonmez & Dogan, 2017). Since the green areas are less in the settlements that have been exposed to the effects of urbanization, it prevents the infiltration of precipitation into the soil. For this reason, the risk of flooding in cities may increase six times (Uzuntaş & Özturk, 2019). There were 111 floods in Turkey between the years 1989-1998. A total of 306 people lost their lives in these floods. 255,640 hectares of agricultural land were flooded, and the total property damage was US$ 1,935.4 million (Kopar et al., 2011).

Sakarya River Basin in Turkey is a region where frequent floods occur, and it is in the status of a risky area in terms of floods. Karasu is located at the mouth of the Sakarya River, where flows into the Black Sea. Karasu is a region with high economic value due to its port, industrial area, and fertile agricultural lands (Dogan et al., 2013). For this reason, it is necessary to obtain flood hazard maps of the region.

Between 0-8 km from the mouth of the river, there was an increase of 1 m due to the accumulation in the thalweg elevation and a decrease of 7 m due to the scour of the thalweg elevation between 8-84 km (Işık et al., 2006). Although the three dams located on the Sakarya River seem to control the sediment movement, the effects of the flow discharged by the closest dam, which is 150 km away from the mouth of the river, are reflected up to the mouth of the river.

Since 1965, the Sakarya River bed has expanded due to scour, and the water level and depth in the river have decreased, except for the first 10 km from the Black Sea (Sonmez & Dogan, 2017; Uzuntaş & Özturk, 2019). The main reason for these changes is that incoming solids are kept in the reservoir by the dams built on the river bed and cannot reach the downstream of the dam. Thus, since the solid material carried in the downstream section is larger (Qst>Qsg) than the solid material coming in, it shows that scours occur in the river downstream (Rupal& Agnihotri, 2019; Sonmez & Dogan, 2017). In other words, clean water with a high carrying capacity left from the dam causes scour of downstream. After the dams, some of the amounts of suspension material carried by the river were fed by scour from the river bed.

Besides the dam effect, there has been commercial sand extraction in the Sakarya River in the last 30 years. Sand extraction both carves the river bed and makes the river bed suitable for carving with the river flow. The sediment carried along the river accumulates due to the decrease in flow velocity and carrying capacity as it approaches the river mouth and closes the riverbed, causing the flow to swell backward and causing coastal flooding.

The devastating effects of river floods can be predicted by the results of finite difference hydrodynamic models for estimating and mapping flood hazards. Flood hazard maps allow for disaster preparedness and response. Flood mapping is essential for land use planning and disaster management in areas with a high probability of flooding. On the other hand, reliable and rapid flood forecasting tools are necessary to develop adequate emergency response strategies and to prevent impacts and mitigate catastrophic effects (Dottori et al., 2016). The first step in the preparation of hazard maps is to create a data collection digital elevation model (Prinos, 2008). Geographical information systems and remote sensing techniques are used to collect and process the data needed in flood disaster forecasting (Yanmaz, 2007).

Many programs are used in flood mapping. Hydrological Engineering Center-River Analysis System (HEC-RAS), one of the software packages developed by the US Army Corps of Engineers and using physically-based equations, is one of the most well-known and widely used programs in scientific literature and practice (HEC-RAS, 2021). It offers the opportunity to model in 2D.

In this study, instead of HEC-RAS 1D hydraulic modeling, 2D HEC-RAS hydraulic modeling is used. Because the 1D method is weak in calculating the multidirectional flood wave propagation, on the other hand, 2D hydraulic models are the most suitable solution for simulating flood wave lateral diffusion (Costabile et al., 2020). The 2-dimensional analysis of river floods caused by estuary blockages is not a very common study in the literature. The studies in the literature are generally addressed within the scope of the exposure of the river bed to flows above its capacity and the inadequacy of the capacities of hydraulic structures (Barredo, 2009; Bouwer et al., 2010; Kreft, 2011; United Nations Office for Disaster Risk Reduction, 2011; Barredo et al., 2012; Quiroga et al., 2016; Lim & Brandth, 2019; Merwade et al., 2008; Pinos & Timbe, 2019). Studies on the determination of flood risk due to river mouth blockage are limited and there are none for the study area. In this respect, the study is unique and deals with the relationship between sediment transport and flooding.

2. Methodology

2.1. Study Area

Karasu district is an important region in terms of economic development impact for the Eastern Marmara region due to reasons such as the Black Sea trade port, industrial facilities, and tourism investments. The regional settlement distribution is concentrated in the region close to the Black Sea coastline and the Black Sea trade port.

On the other hand, the Sakarya River flows through this residential area and empties into the Black Sea. As the study area, a river length of 10 km was determined from downstream of the Sakarya River. This region was determined by taking into account the changes in river morphology, topography, and population distribution. The study area is approximately 22.38 km^2. The river width varies between 180 m and 40 m. On average, the width of the river can be considered as 100 m. The depth of the river from thalweg varies from 3 m to 5 m along the river. There are four water channels in total, one from the district center and 3 to be used in fields and gardens, with an estimated average width of 10 m, which are connected to the river. These channels are also included in the terrain model as they can act as a drain and may affect the hydraulic modeling.

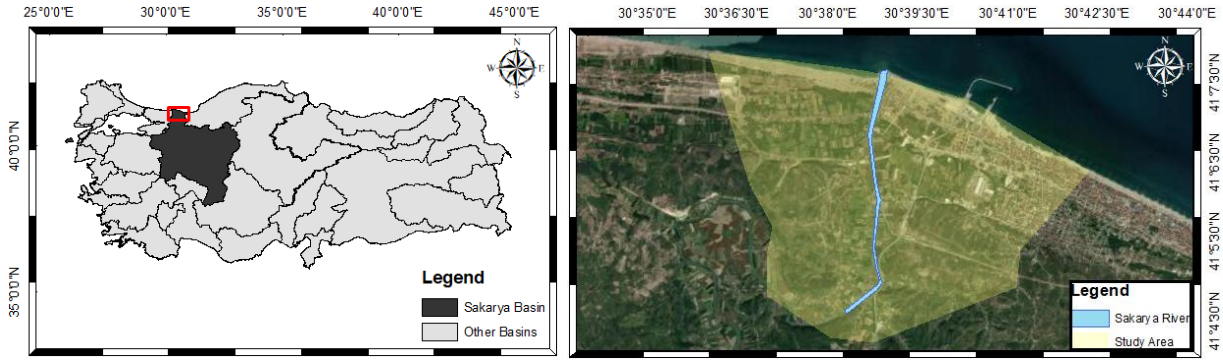

Figure 1: Sakarya River Basin and Karasu region

In Figure 1, the study area is located between latitude $30^0$35'0"E-$30^0$45'0"E and longitude $42^0$8'0"N-$41^0$4'0"N according to topographic region maps and region satellite images. The flood risk analyses in this study area were made according to the flow diagram in Figure 2.

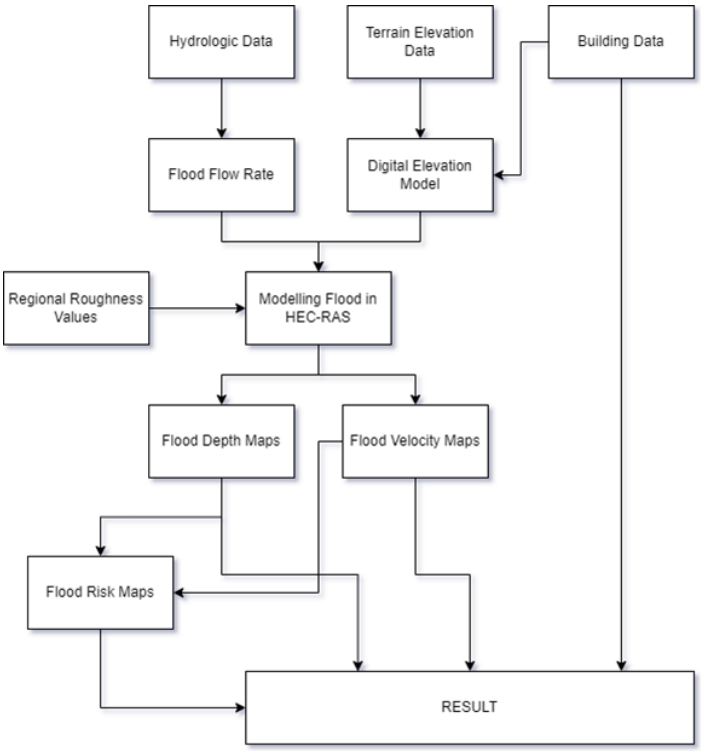

Figure 2: Flow diagram for flood risk analysis

2.2. Manning Roughness Data

The 2018 land use map from the EEA data pool was applied to create the Manning roughness map of the research area. The land use classification on the map determines the CLC code that has been assigned. The manning values chosen to correspond with these codes are also listed in Table 1. The regional roughness map was produced by importing the data from Table 1 and Figure 3 into the CLC land use map.

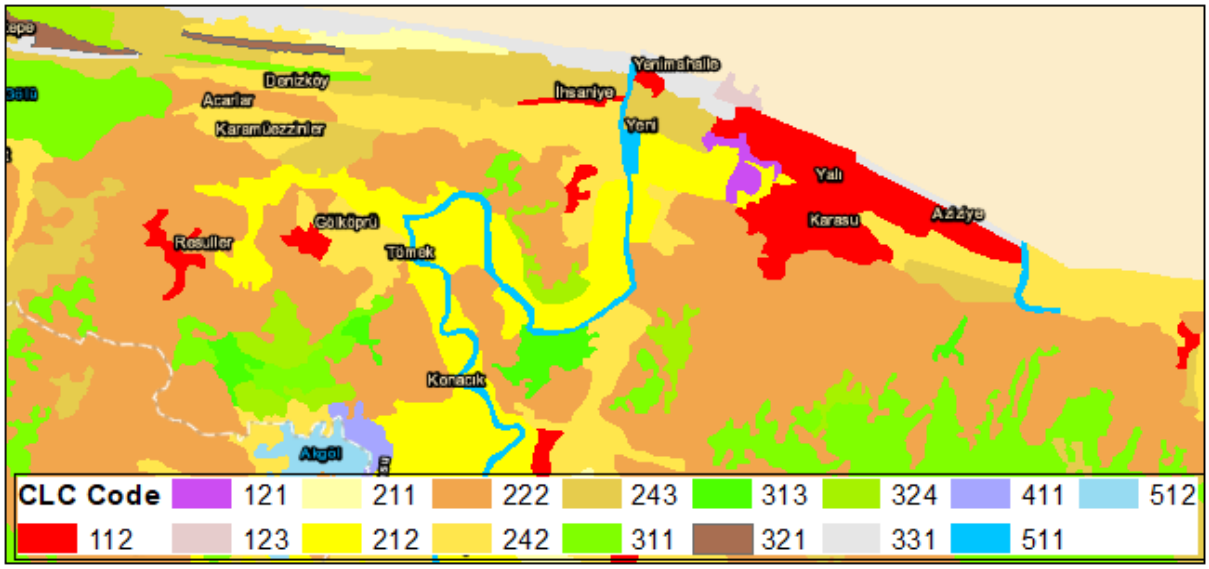

Figure 3: Corine land use map

Table 1: Manning roughness values (Copernicus Land Monitoring Service, 2018)

CLC Code	Label	Manning Values
112	Discontinuous urban fabric	0.013
121	Industrial or commercial units	0.013
123	Port areas	0.013
211	Non-irrigated arable land	0.03
212	Permanently irrigated land	0.03
222	Fruit trees and berry plantations	0.08
242	Complex cultivation patterns cultivation patterns	0.04
243	Land principally occupied by agriculture, with significant areas of natural vegetation	0.05
311	Broad-leaved forest	0.1
313	Mixed forest	0.1
321	Natural grasslands	0.04
324	Transitional woodland-shrub	0.06
331	Beaches, dunes, sands	0.025
411	Inland marshes	0.04
511	Water courses	0.05
512	Water bodies	0.05

2.3. Hydrological Data for Upstream Boundary Condition

Due to the missing flow records of the Sakarya River, the flood flow rates for different recurrences were calculated using deterministic methods depending on the extreme precipitation for the recurrent flood flow.

In the study, calculations were made with the data taken from the observation station of Sakarya province. The extreme precipitation data between 1929 and 2015 are as in Figure 4.

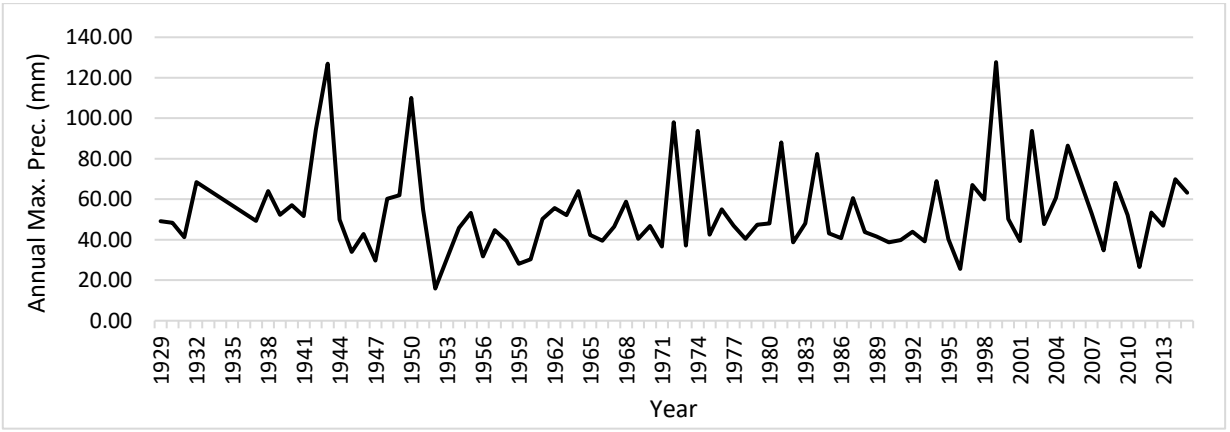

Figure 4: Variation of precipitation over the years

Considering the basin precipitation area, the extreme distribution of annual maximum precipitation was calculated by different methods in the calculation of recurrent flood flow and hydrographs. To choose between the methods, the Kolmogorov-Smirnov method was tested. The Log-Pearson Type III method was determined as the distribution type with the most optimum results. The Non-Superposed Mockus Method was used to calculate the recurrent flood flow with the Log-Pearson Type III distribution. The reason for using the non-superposed Mockus method is that it gives effective and accurate results in basins where precipitation concentration time is less than 30 hours. Also, in the FEMA 17/B bulletin, it was stated that Log-Pearson Type III distribution should be used in the calculation of recurrence flood flow. The results given according to the Kolmogorov-Smirnov Test Method also gave values that support the criteria specified in the literature. In the Mockus method, hydrographs are triangular in shape and are preferred due to their ease of calculation and drawing (Koca, 2014; Çıtakoğlu et al., 2017). This method can be applied in regions where there is no current observation station or there is no recorded data based on long years. In the Mockus (non-superposite) method, it can be used in drainage basins where the collection time (t_c) is <30 hours. If t_c is greater than 30 hours, the drainage area is divided into secondary parts. The hydrographs to be drawn separately for each subdivided area are superposed by considering the delay times.

The flood flow values calculated according to these methods are given in Table 2. According to the Kolmogorov-Smirnov Test Method, the significance values of the Log-Pearson Type-3 distribution calculation are acceptable (Table 3).

Table 2: Return period discharges

	2	**5**	**10**	**25**	**50**	**100**	**200**	**500**
Normal	50.14	70.85	81.68	93.23	100.68	107.38	113.50	120.88
Log-Normal II	45.02	66.55	81.64	101.53	116.85	132.63	148.86	171.11
Log-Normal III	47.71	69.60	82.61	97.84	108.45	118.58	128.32	140.74
Pearson III	45.21	68.04	83.10	101.68	115.12	128.19	140.98	153.78
Log-Pearson III	49.89	68.00	80.46	96.73	109.19	122.01	135.25	149.92
Gumbel	44.07	69.15	85.76	106.75	122.32	137.77	153.16	173.48

Table 3: Kolmogorov-Smirnov test results

	Theoric P	**Empirical P**	**Max. P Δmax**	**Measured P**	**Significance Percentages**				
					0.80	*0.85*	*0.90*	*0.95*	*0.99*
Normal	0.679	0.136	0.184	38.7	Reject	Reject	Reject	Reject	Reject
Log-Normal II	0.628	0.136	0.236	38.7	Reject	Reject	Reject	Reject	Reject
Log-Normal III	0.653	0.136	0.211	38.7	Reject	Reject	Reject	Reject	Reject
Pearson III	0.376	0.136	0.240	38.7	Reject	Reject	Reject	Reject	Reject
Log-Pearson III	0.242	0.136	0.105	38.7	Accept	Accept	Accept	Accept	Accept
Gumbel	0.413	0.136	0.277	38.7	Reject	Reject	Reject	Reject	Reject

Different recurrent flood flow rates Q_{500}, Q_{100}, Q_{50}, Q_{25}, Q_{10}, Q_5, Q_2 were calculated by synthetic methods and the flood hydrographs are as in the Figure 5 below.

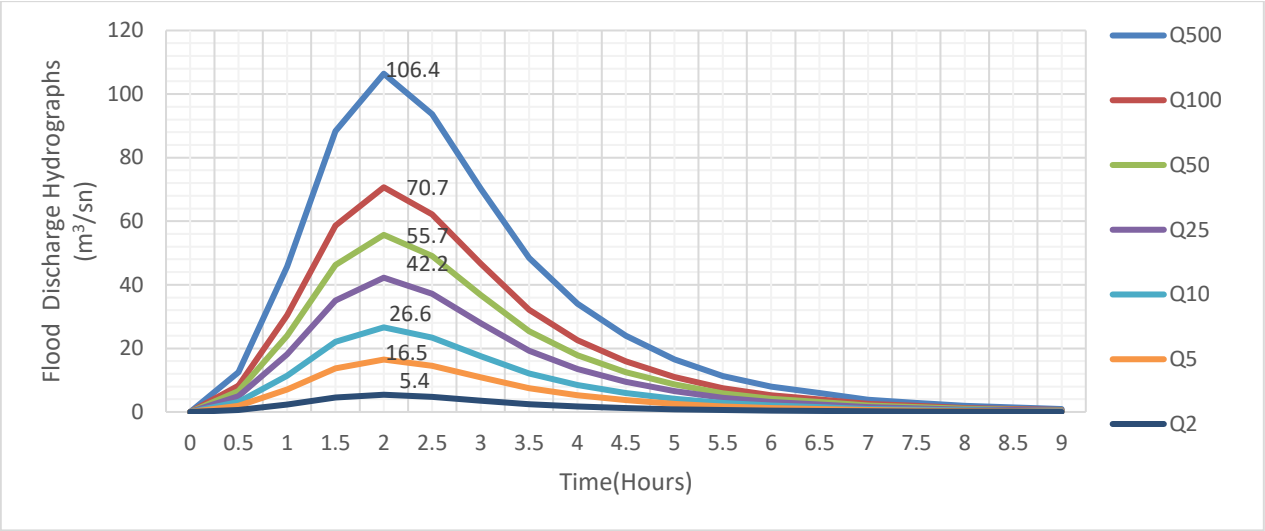

Figure 5: Flood hydrographs for different recurrent flood flows

2.4. Sediment Data for Downstream Boundary Condition

As a result of sediment transport in streams, the economic life of the structures on the stream is reduced due to sedimentation in their reservoirs, and it also damages agricultural areas due to erosion of the top layer, which is the most productive part of the soil. In addition, estimations of sediment transport amount have an important place in river transport, flood control, in the selection of types and locations of hydroelectric power plants, in terms of determining the amount of scour or piling up and taking the necessary precautions. The sediment movement of the Sakarya River is quite high due to its length, basin shape, and soil characteristics. However, after the dams built on the Sakarya River, a decrease was observed in the amount of sediment transport downstream of the river. Because the dam reservoir has stopped the sediment movement due to sedimentation. With the retention of the sediment by the dam, the clean water, whose energy increases in the downstream part, creates scour (Işık et al., 2006).

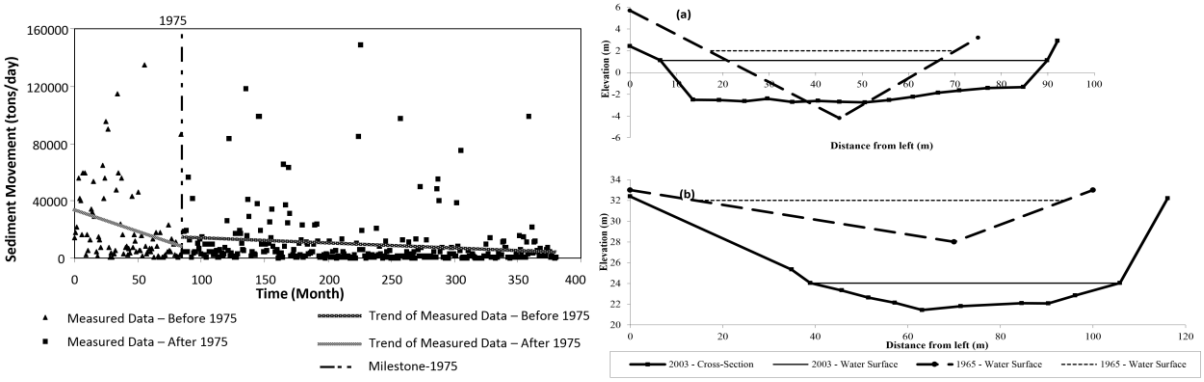

Figure 6: Differences in bathymetry by years (Işık et al., 2006)

The trend of suspended sediment amount for before and after 1975 was examined and it is understood that it has a decreasing trend. The average flow between 1964 and 1974 is 197.32 m^3/s and the daily suspended sediment transport is 21490 tons. Between 1975 and 1999, the average flow was 157.4 m^3/s and the daily suspension material transport was 9500 tons (Figure 6).

Cross-sections measured from the 8th and 84th km of the river in 1965 and 2003 are given in Figure 5, respectively. While accumulations occur at the mouth of the river, scour continue increasingly towards the downstream. There was a 1 m increase (accumulation) in the thalweg elevation at the 8th km from the river mouth, and a 7 m scour of the thalweg elevation at the 84th km. The riverbed has widened since 1965, except for the first 10 km from the mouth, the water level and depth in the river have decreased (Işık et al., 2006).

This causes the flow velocity to decrease and sedimentation to accumulate at the river mouth. Accumulations at the river mouth cause floods.

In this study, the effect of upstream flood risk due to blockage of the river mouth due to sediment transport and accumulation, preventing the discharge of the flow, will be investigated.

2.5. Digital Elevation Model

In 2-dimensional flood models, it is necessary to represent the effect of structures that cause sudden height changes such as buildings and walls, which are frequently encountered in residential areas. Because, unless the obstacles to the physical progress of water on the land are defined in the model, realistic analysis cannot be made. This is one of the biggest differences between two-dimensional analysis and one-dimensional analysis, which affects the result. In one-dimensional analysis, the accuracy rate decreases because it calculates the flow between the section that coincides with the structure and the sections before and after it, and calculates it according to the average height. In the two-dimensional analysis, since the calculation is made according to the interaction of the mesh with the neighboring meshes, if the terrain model and boundary conditions are correct, the error rate due to elevation is very low. In the study area, a digital elevation model was created with 0.5-metre precision obtained from the Sakarya Metropolitan Municipality. Buildings were added to the raster data, resulting in a comprehensive representation of the terrain (Figure 7).

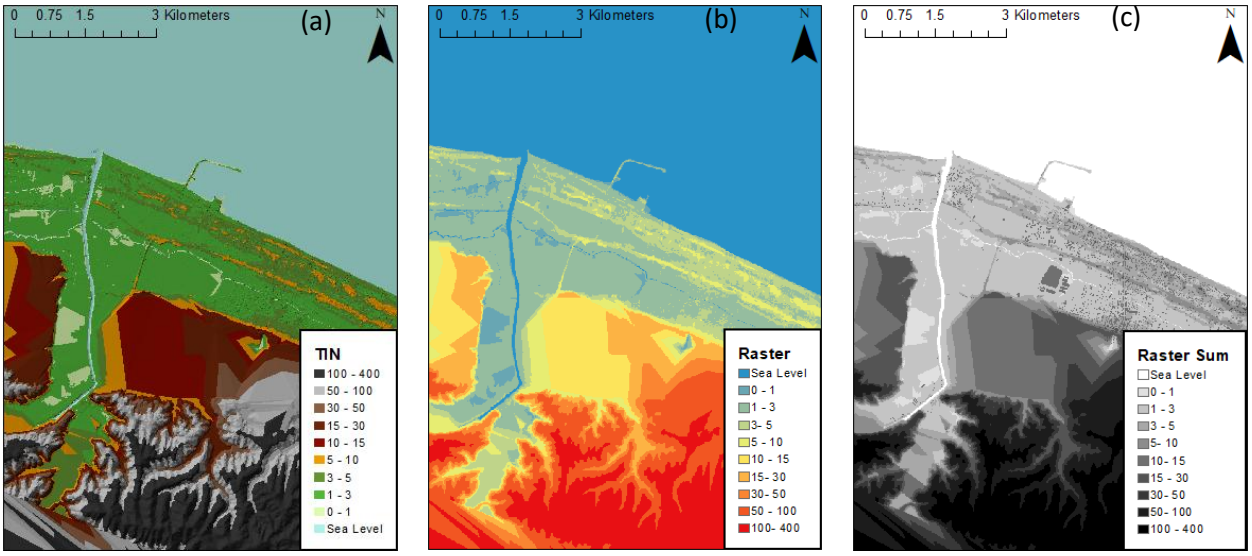

Figure 7: a) TIN, b) raster, and c) modified Digital Elevation Model

2.6. Hydraulic Model

The hydraulic model was created with the HEC-RAS 6.1 program. The HEC-RAS program is used for river hydraulic analysis, graphical representation, flood and flood propagation animation. This program can simulate one-dimensional and two-dimensional or combined-dimensional flow in open channels (Zelenakova et al., 2018). 2-dimensional flood analysis was used in this study. In the HEC-RAS program, the region is divided into square areas (smallness of the square areas increases the study detail) and a 2-dimensional flood analysis is performed above the water depth, velocity and lateral variability. It is recommended to enter precipitation as effective precipitation, as the program does not take into account soil infiltration and other losses (Zeiger & Hubbart, 2021; Urzică et al., 2021).

Although the 1D model is the same with the principles of conservation of mass and momentum, the 2D flow changes over time in 2D spatial dimension. The 2-dimensional continuity equation is as follows (Betsholtz & Nordlöf, 2017):

$$\frac{\partial \mathrm{H}}{\partial \mathrm{t}} + \frac{\partial(\mathrm{hu})}{\partial \mathrm{x}} + \frac{\partial(\mathrm{hv})}{\partial \mathrm{y}} + \mathrm{q} = 0 \tag{1}$$

In equation 1, H is the water surface elevation, h is the water depth, the mean velocity depths in the u and v, x and y directions, and q is the unit discharge. The 2-dimensional momentum equation is in the x direction in equation 2 and in the y direction in equation 3.

$$\frac{\partial \mathrm{u}}{\partial \mathrm{t}} + \mathrm{u}\frac{\partial \mathrm{u}}{\partial \mathrm{x}} + \mathrm{v}\frac{\partial \mathrm{u}}{\partial \mathrm{y}} = -\mathrm{g}\frac{\partial \mathrm{H}}{\partial \mathrm{x}} + v_t\left(\frac{\partial^2 u}{\partial x^2} + \frac{\partial^2 u}{\partial y^2}\right) - c_f u + fv \tag{2}$$

$$\frac{\partial \mathrm{u}}{\partial \mathrm{t}} + \mathrm{u}\frac{\partial \mathrm{u}}{\partial \mathrm{x}} + \mathrm{v}\frac{\partial \mathrm{u}}{\partial \mathrm{y}} = -\mathrm{g}\frac{\partial \mathrm{H}}{\partial \mathrm{y}} + v_t\left(\frac{\partial^2 u}{\partial x^2} + \frac{\partial^2 u}{\partial y^2}\right) - c_f u + fv \tag{3}$$

In these equations, H represents the water surface elevation, vt is the eddy viscosity coefficient, c_f is the friction coefficient, f is the Coriolis parameter, v and u are the mean velocity depths in x and y directions.

3. Results and Discussion

It can define flood risk as the probability that parameters such as life and property safety will be affected by flood waters in a certain area, within a certain period. There is an inverse relationship between the water level and the probability of its occurrence. That is, the probability of occurrence of high water levels is lower than that of shallow water levels. As long as it does not exceed natural levees or flood walls, there is a relationship between the water level and the return period. According to conventional 1D flood maps, for such a situation, the flood risk of all lands below the waterline is at the same level as the flood wall risk, so there is an assumption that if this level is exceeded, the entire land will be at risk. This approach does not take into account the spread of the runoff and all land below the waterline is designated as at risk of flooding without grading. The flood will not immediately spread over the entire land. It will take time to propagate into the inundation area. How long it will take depends on the extent of the water, the character of the land, the roughness of the land cover, and the presence of obstructions such as buildings. This time component is of great importance for decision-makers. While some people will be faced with the risk of flooding within a few hours, for others, this risk will become a danger after days. Decision makers need to know in advance which people should be evacuated first and which roads are available. As 1D flood maps identify flood areas on a cross-sectional basis, they are unable to provide the requisite accurate information to develop such regional plans. In addition, it will not be beneficial in making these plans for possible future floods. In this study, the HEC-RAS program, which is used for two-dimensional hydrodynamic modeling, has been developed for 2-dimensional comprehensive analysis. It is used in many hydraulic analyses such as tides, dam failure, and flood waves. The model simulates the change of flow and water level due to various forces. Water levels and flows are analyzed for meshes within the defined area, with determined bathymetry, bed roughness coefficient, wind field, and hydrographic boundary conditions. The modeling system analyzes according to the full-time and non-linear continuity and conservation of momentum equations. The output of the simulation is the water level and the water velocity. The model simulates 2D unsteady flows of laminar and turbulent fluids. Continuity and momentum equations are solved for each mesh in the study area using the finite difference method.

As mentioned, a model boundary was determined to cover possible areas of flood inundation and this study area was divided into meshes. For the land cover roughness values, the roughness data with the same mesh resolution was also prepared and superposed with the digital elevation model. Upstream and downstream boundary conditions are determined and defined in the model. The flood hydrograph, which indicates the time-flow relationship of the calculated recurrent flood flows, was defined in the model as an upstream boundary condition. Also, the downstream boundary condition was defined as the limited flow resulting from the blockage of the river mouth due to sediment accumulation. The model was analyzed for different recurrences and inundation, depth, and water velocity were determined for each mesh. The areal distributions are given in Figure 8.

Since flood inundation was not observed outside the river for Q_2 and Q_5 flows, the flood depth and water velocity maps of the flow hydrographs in these recurrence were not included.

Figure 8: Depth (m) and velocity (m/s) maps of different recurrence

Flood depths vary depending on topography. The depth is quite high in the region close to the river banks and in the places where the elevation is low. As a result of the flood analysis, it was determined that the inundation areas for the 500, 100, 50, 25, and 10-year repeated flood analyses of the Sakarya River were 5.37 km^2, 2.57 km^2, 1.75km^2, 1.72km^2, and 0.67 km^2, respectively. It was determined that the depth of the flood varied between 8.63 m and 1.00 m for the 500-year recurrence with the highest flood inundation. For all recurrence intervals, it was determined that the flood depths were higher in the upstream part of the study area depending on the topography. It was determined that the spread occurred due to accumulation in the plain area, close to the river mouth, where the city center is located.

The flood hazard is directly proportional to the flood depth and water velocity. The hazard rating was evaluated according to these two factors. The limit ranges of the parameters used in the hazard rating are given in the table. Boundary intervals were calculated using the minimum and maximum values of depth and velocity (Alphen et al., 2009).

The hazard rating is set at five levels, from very low to very high hazard. Using the created water depth and water velocity maps, raster superposition operations were performed with the raster calculator module of the ArcGIS program (Table 4). Accordingly, the areal graded hazard maps for 10, 25, 50, 100, and 500-year recurrent floods are given in Figure 9.

Table 4: Flood hazard rating parameters (Alphen et al., 2009)

Hazard Levels	a : Depth (m)		b : Velocity (m/s)		Danger=a*b	
	min	max	min	max	min	max
Extreme Low Hazard	0	0.25	0	0.5	0	0.125
Low Hazard	0.25	0.5	0.5	1	0.125	0.5
Moderate Hazard	0.5	0.75	1	1.25	0.5	0.9375
High Hazard	0.75	1	1.25	1.75	0.9375	1.75
Extreme High Hazard	1	Max	1.75	Max	1.75	Max

Figure 9: Flood hazard maps

Sakarya River recurrent flood inundation maps have been examined and it has been determined that it can carry the 2 and 5-year flood recurring flows. In other words, the stream cross-section is sufficient for these flood flows. The flood inundation map of the 10-year recurrent flood flow rate was examined; It is seen that the flood waters that spread over 1.3 km^2 of agricultural area in the left floodplain of the river between 1-2,3 km affect a small number of residences in the fields. The flood inundation map of 25 years of recurrent flood flow has been examined; It is seen that 2.3 km^2 of agricultural area and a few houses in the floodplain of the river between 0-4.5 km have been affected by the flood (Figure 10). The flood inundation map of the 100-year recurrent flood discharge was evaluated; In addition to the 50-year hazard map, the flood appears to have affected residential areas in the left overbank section. It is seen that the irrigation channels passing through this region are effective in the discharge of the flood. In addition, it was determined that many houses were affected by the flood. The flood inundation map of 500 years of recurrent flood flow was analyzed; It was determined that the flood caused a spread over an area of 7.4 km^2, and the extent and flow depth increased in the left overbank section. It is seen that the residences in the Karasu district center are not affected by this flood.

According to the 500-year recurrent hazard distribution in the floodplain; 5 houses are as an Extreme High Hazard, 11 houses are as High Hazard, 49 houses are as Moderate Hazard, 104 houses are as Low Hazard, and 347 houses are as an Extreme Low Hazard were determined.

Figure 10: Percentage information on flood modeling for different return period discharges

4. Conclusion

The findings of the study on the flood risk due to sediment accretion and considering the economic value of the region, it is considered that possible risks may have negative effects on the country's economy. For this reason, it is necessary to prevent the occurrence of floods due to sediment transport in the region. For this, scours should be prevented by constructing sediment traps in the river bed downstream of the dam. In this way, sedimentation occurring at the river mouth will be prevented. If the carrying capacity of the river is sufficient, it will prevent flooding. In addition, the Black Sea wave height and intensity are very high, causing momentum forces to arise at the mouth of the river and forcing the sea discharge. For this reason, the momentum force effect should be eliminated with offshore breakwaters constructed parallel to the river mouth.

5. Acknowledgment

This article was produced from the project titled; "Creating Flood Inundation Maps of Karasu County of Sakarya Province and Investigating The Risk-Damage Status of The Region According to Different Scenarios", Project No. 2020/AP/0003, supported by Yalova University Scientific Research.

References

Alfieri, L., Bisselink, B., Dottori, F., Naumann, G., Roo, A. de, Salamon, P., Wyser, K., & Feyen, L. (2017). Global projections of river flood risk in a warmer world. *Earth's Future, 5*(2), 171–182. https://doi.org/10.1002/2016EF000485

Alphen, J. V., Martini, F., Loat, R., Slomp, R., & Passchier, R. (2009). Flood risk mapping in Europe, experiences and best practices. *Journal of Flood Risk Management, 2*(4), 285–292. https://doi.org/10.1111/j.1753-318X.2009.01045.x

Barredo, J. I. (2009). Normalised flood losses in Europe: 1970–2006. *Natural Hazards and Earth System Sciences, 9*(1), 97–104.

Barredo, J. I., Saurí, D., & Llasat, M. C. (2012). Assessing trends in insured losses from floods in Spain (1971–2008). *Natural Hazards and Earth System Sciences, 12*(5), 1723–1729. https://doi.org/10.5194/nhess-12-1723-2012

Betsholtz, A., & Nordlöf, B. (2017). *Potentials and limitations of 1D, 2D and coupled 1D-2D flood modelling in HEC-RAS: A case study on Höje River* [Master thesis, Lund University]. https://www.lunduniversity.lu.se/lup/publication/8904721

Birkholz, S., Muro, M., Jeffrey, P., & Smith, H. M. (2014). Rethinking the relationship between flood risk perception and flood management. *Science of The Total Environment, 478*, 12–20. https://doi.org/10.1016/j.scitotenv.2014.01.061

Bouwer, L. M., Bubeck, P., & Aerts, J. C. J. H. (2010). Changes in future flood risk due to climate and development in a Dutch polder area. *Global Environmental Change, 20*(3), 463–471.

Bubeck, P., Otto, A., & Weichselgartner, J. (2017). Societal impacts of flood hazards. *Oxford Research Encyclopedia of Natural Hazard Science*. https://doi.org/10.1093/acrefore/9780199389407.013.281

Copernicus Land Monitoring Service. (2018). *CORINE Land Cover 2018 (vector/raster 100 m), Europe, 6-yearly*. Retrieved from https://land.copernicus.eu/en/products/corine-land-cover/clc2018

Costabile, P., Costanzo, C., Ferraro, D., Macchione, F., & Petaccia, G. (2020). Performances of the new HEC-RAS version 5 for 2-D hydrodynamic-based rainfall-runoff simulations at basin scale: Comparison with a state-of-the-art model. *Water, 12*(9), Article 2326. https://doi.org/10.3390/w12092326

Çıtakoğlu, H., Demir, V., & Haktanır, T. (2017). L-momentler yöntemiyle Karadeniz'e dökülen akarsulara ait yıllık anlık maksimum değerlerin bölgesel frekans analizi. *Niğde Ömer Halisdemir Üniversitesi Mühendislik Bilimleri Dergisi, 6*(2), 571–580.

Dogan, E., Sönmez, O., Yapan, E., & Othan, K. (2013). Aşağı Sakarya Nehrinde taşkın yayılım haritalarının elde edilmesi. *Sakarya University Journal of Science, 17*(3), 363–369. https://doi.org/10.16984/saufbed.44256

Dottori, F., Salamon, P., Bianchi, A., Alfieri, L., Hirpa, F. A., & Feyen, L. (2016). Development and evaluation of a framework for global flood hazard mapping. *Advances in Water Resources, 94*, 87–102. https://doi.org/10.1016/j.advwatres.2016.05.002

HEC-RAS. (2021, June 14). *Hydrologic Engineering Center's (CEIWR-HEC) River Analysis System (HEC-RAS)*. Retrieved from https://www.hec.usace.army.mil/software/hec-ras/

Işık, S., Şaşal, M., & Doğan, E. (2006). Sakarya Nehrinde barajların mansap etkisinin araştırılması. *Gazi Üniversitesi Mühendislik Mimarlık Fakültesi Dergisi, 21*(3), 401–408.

Jongman, B. (2018). Effective adaptation to rising flood risk. *Nature Communications, 9*, Article 1986. https://doi.org/10.1038/s41467-018-04396-1

Koca, Y. C. (2014). *Rize İyidere alt havzası İkizdere kesiti için birim hidrografın belirlenmesi* [Uzmanlık tezi, T.C. Orman ve Su İşleri Bakanlığı]. https://kutuphane.tarimorman.gov.tr/vufind/Record/1181327

Kopar, İ., Polat, S., Hadimli, H., & Özdemir, M. (2011). 4-6 Mart 2004 Pulur Çayı (Ilıca-Erzurum) sel-taşkın afeti. *Doğu Coğrafya Dergisi, 10*(13), 187–218.

Kreft, M. (2011). *Quantifying the impacts of climate-related natural disasters in Australia and New Zealand*. Munich Re, Wellington.

Lim, N. J., & Brandt, S. A. (2019). Flood map boundary sensitivity due to combined effects of DEM resolution and roughness in relation to model performance. *Geomatics, Natural Hazards and Risk, 10*(1), 1613–1647.

Merwade, V., Olivera, F., Arabi, M., & Edleman, S. (2008). Uncertainty in flood inundation mapping: Current issues and future directions. *Journal of Hydrologic Engineering, 13*(7), 608–620.

Pinos, J., & Timbe, L. (2019). Performance assessment of two-dimensional hydraulic models for generation of flood inundation maps in mountain river basins. *Water Science and Engineering, 12*(1), 11–18.

Prinos, P. (2008). Review of flood hazard mapping. *Global NEST Journal, 13*(3), 193–214.

Quiroga, V. M., Kure, S., Udo, K., & Mano, A. (2016). Application of 2D numerical simulation for the analysis of the February 2014 Bolivian Amazonia flood: Application of the new HEC-RAS version 5. *Ribagua, 3*(1), 25–33.

Rupal, K. W., & Agnihotri, P. G. (2019). Flood risk assessment and resilience strategies for flood risk management: A case study of Surat City. *International Journal of Disaster Risk Reduction, 40*, Article 101155. https://doi.org/10.1016/j.ijdrr.2019.101155

Sonmez, O., & Doğan, E. (2017, September 29 – October 1). *Asi Nehri yatağının taşkın taşıma kapasitenin belirlenmesi* [Conference presentation]. 5th International Symposium on Innovative Technologies in Engineering and Science, Baku, Azerbaijan.

United Nations Office for Disaster Risk Reduction. (2011). *Global Assessment Report on Disaster Risk Reduction – Revealing Risk, Redefining Development.* United Nations, Geneva.

Urzică, A., Mihu-Pintilie, A., Stoleriu, C. C., Cîmpianu, C. I., Huţanu, E., Pricop, C. I., & Grozavu, A. (2021). Using 2D HEC-RAS modeling and embankment dam break scenario for assessing the flood control capacity of a multi-reservoir system (NE Romania). *Water, 13*(1), Article 57. https://doi.org/10.3390/w13010057

Uzuntaş, Ö., & Öztürk, S. (2019). An assessment on the flood and flash flood regulations in Turkey: A comparison with different countries and legal deficiency analysis. *Journal of International Scientific Research, 4*(2), 146–159. https://doi.org/10.23834/isrjournal.520732

Yanmaz, A. M. (2007, May 28–29). *Akarsu geçişlerinde taşkın kaynaklı problemlerin değerlendirilmesi* [Bildiri Sunumu]. Sel-Heyelan-Çığ Sempozyumu, Samsun, Türkiye.

Zeiger, S. J., & Hubbart, J. A. (2021). Measuring and modeling event-based environmental flows: An assessment of HEC-RAS 2D rain-on-grid simulations. *Journal of Environmental Management, 285*, Article 112125. https://doi.org/10.1016/j.jenvman.2021.112125

Zelenakova, M., et al. (2018). Flood risk modelling of the Slatvinec stream in Krušlov village, Slovakia. *Journal of Cleaner Production, 212*, 109–118. https://doi.org/10.1016/j.jclepro.2018.12.008